Astron. Astrophys. 242, 27–34 (1991)

ASTRONOMY AND ASTROPHYSICS

X-ray observations of the broad line radio galaxy 3C 382: variability, an iron line and soft X-ray emission

J.S. Kaastra[1], H. Kunieda[2], and H. Awaki[2]

[1] SRON Laboratory for Space Research, P.O. Box 9504, NL-2300 RA Leiden, The Netherlands
[2] Department of Astrophysics, School of Science, Nagoya University, Furo-cho, Chikusa-ku, Nagoya 464-01, Japan

Received May 2, accepted July 26, 1990

Abstract. A long Ginga observation of the broad line radio galaxy 3C 382 shows low amplitude X-ray variability with a characteristic time scale of 2 days. No evidence for variability with rms amplitudes larger than 4% on shorter time scales is found. The X-ray flux was 50% below the minimum of 30 previous detections. The variability amplitude as deduced from this and previous observations increases up to at least a time scale of one year. Identifying the minimum and maximum variability time scales with the thermal and viscosity time scale in an accretion disk around a massive black hole, a central mass of $\sim 10^8\ M_\odot$ and an accretion rate of $\sim 0.1\ M_\odot\ \mathrm{yr}^{-1}$ results. These parameters are also consistent with the UV continuum spectrum.

We report for the first time an Fe-fluorescence line in 3C 382. The line energy reduced to the rest frame of 3C 382 is 6.52 ± 0.27 keV, consistent both with cool or hot material. The line equivalent width of 280 eV is very high. This may be either related to the probably large inclination of the accretion disk in 3C 382 or due to time delay effects in combination with the low continuum flux.

The soft excess below 2 keV varies differently from the main power law, but with a similar time scale. Its spectral shape is poorly determined but its temperature of $\sim 5 \times 10^6$ K is much higher than found in previous EXOSAT observations, while its bolometric luminosity is only $\sim 10\%$ of the 2–10 keV luminosity. If this difference with EXOSAT is related to the low flux during the present Ginga observation, a strong anticorrelation between temperature and flux of the soft X-ray excess in 3C 382 is implied.

Key words: active galaxies: X-rays – active galaxies: variability – radio galaxies: X-rays

1. Introduction

1.1. X-ray variability

Gamma rays and X-rays originate closer to the central powerhouse of active galactic nuclei (AGN) than any other part of the electromagnetic spectrum. In particular, the variability time scale for X-rays is much faster than for optical or radio emission. The observed X-ray variability properties may serve to constrain the size and geometry of the central part of the AGN. Furthermore, since a considerable part of the total energy output is produced in the form of X-rays, the X-ray luminosity is an important factor for estimates in which the Eddington luminosity is involved. The X-ray spectrum plays a key role in constraining models with e.g. an accretion disk surrounding the central black hole.

It is well known (Barr & Mushotzky 1986) that the variability time scale is proportional to the X-ray luminosity. This was interpreted as evidence that the emitting plasma is near the limit of being dominated by electron-positron pairs. The luminosity-time scale correlation can be understood if the hard X-ray luminosity scales linearly with the central mass. Observation of fluctuations much faster than predicted by this correlation would imply luminosities close to the Eddington limit thus constraining the geometry of the X-ray source considerably.

We selected candidates for rapid variability using the following constraints. The 2–10 keV X-ray luminosity range was limited by the demand of no internal absorption ($L > 10^{37.5}$ W, cf. Mushotzky 1984) and Barr-Mushotzky variability time scales smaller than a few days ($L < 10^{38}$ W); furthermore, low galactic absorption (column density $< 10^{25}\ \mathrm{m}^{-2}$) and sufficient X-ray flux received at Earth was required (> 0.5 mCrab); out of 5 sources fulfilling these requirements 3C 382 and III Zw 2 were the radio loud sources. Contrary to III Zw 2, both the EXOSAT LE observations of 3C 382 (Barr 1990) and the Einstein IPC and HRI observations (Morganti et al. 1988) showed no evidence for contaminating sources close to 3C 382.

1.2. 3C 382

3C 382 (identical to CTA 80) is one of the nearest broad line radio galaxies (BLRG). With a redshift of 0.0586 (Schmidt 1965) its luminosity distance and angular size distance are 356 and 318 Mpc respectively, using $H_0 = 50\ \mathrm{km\ s^{-1}\ Mpc^{-1}}$ and $q_0 = 0.5$ as throughout this paper.

Radio maps of the source show the typical structure of a double radio source: two oppositely directed lobes at a projected distance of 100 kpc from the optical galaxy (MacDonald et al. 1968), each containing a hot spot near the end (120 kpc) of the jet (Riley & Branson 1973; Burch 1979b; Parma et al. 1986). The energy content of the lobes is at least $2.6\ 10^{51}$ J, while the jets expand probably with a velocity of $1800\ \mathrm{km\ s^{-1}}$, yielding an age for the radio activity of some 70 million years (Burch 1979b). Coinciding with the optical galaxy is a radio core with a flat spectrum (Riley & Branson 1973), which has a diameter of 1.5 pc (Preuss & Fosbury 1983). It varied by 25% on a time scale of 2 yr (Strom et al. 1978).

Send offprint requests to: J.S. Kaastra

The narrow lines originate from an extended (larger than 5 kpc, Yee & Oke 1978) and stratified medium (Osterbrock et al. 1976) which extends at least 25 kpc to the east and 10 kpc to the west (Tadhunter et al. 1986). The rotation curve indicates a mass of $1.5\,10^{11}\,M_{\odot}$ within 10 kpc.

3C 382 has an infrared excess (O'Dell et al. 1978), which from its variability and spectral properties may be identified with thermal reradiation of dust at 1 pc from the nucleus (Puschell 1981). The optical and ultraviolet continuum show evidence for a UV excess (Osterbrock et al. 1976; Yee & Oke 1978) which from its variability properties must originate from a region of at most 1 light year extension (Yee & Oke 1981).

3C 382 is in particular peculiar because of its extremely broad lines: the full width at zero intensity is 25 000 km s^{-1} for the Balmer lines (Osterbrock et al. 1975), and probably up to 30 000 km s^{-1} for the UV lines (Tadhunter et al. 1986). The broad line profiles have a rather complicated and variable structure (Osterbrock et al. 1976; Yee & Oke 1981; Reichert et al. 1985; Tadhunter et al. 1986). The variability properties indicate a radius of the broad line region smaller than $1.3\,10^{15}$ m.

3C 382 was identified with the hard X-ray source H1832+32 (HEAO-1 A-2) by Marshall et al. (1978). It was later reobserved by Einstein and EXOSAT. The EXOSAT observations showed a doubling time of the X-ray flux of 3 days (Barr & Mushotzky 1986), consistent with the general correlation of X-ray luminosity with variability time scale for Seyferts and QSO's.

2. Observations

2.1. Data selection

The present observations of 3C 382 were obtained by the Large Area Counter (LAC) on the third Japanese X-ray astronomy satellite Ginga. The LAC comprises eight multi-cell proportional counters with a total effective area of 4000 cm^2, covering the energy range 1–37 keV (the detection efficiency near those limits is a few percent). The energy resolution is 18% at 6 keV, and scales as $E^{-0.5}$ over the full energy range. The detector has a field of view of $1^\circ \times 2^\circ$ full width at half maximum, and was used in the MPC-1 mode with a time resolution of 16 s. More details about the instrument are given by Turner et al. (1989). A full discussion about the background determination method is given by Hayashida et al. (1989).

3C 382 was observed from 20–23 July 1989. The background spectra were obtained on 19 July 1989 from a region 8° away from 3C 382 and centered at galactic longitude 270.5° and latitude 31.3°.

The detectors consist of two layers, called top and mid layer. We used only data from the top layer, since the mid layer is mostly sensitive to X-ray photons above 10 keV and 3C 382 had a rather low count rate above 10 keV during our observation. The criteria used for inclusion of the data in our spectral and timing analysis were (more details and definitions are given by Hayashida et al. 1989):

1. Surplus over Upper Discriminator (SUD) count rate <8000 counts/128 s. The SUD count rate is the number of X-ray-like events above 24 keV and is a measure of the internal background because the detection efficiency for genuine X-rays is very low ($<6\%$) at such high energies.
2. charged particle cutoff-rigidity (COR) ≥ 9 GeV/c
3. Earth elevation angle $\geq 5^\circ$
4. first and last bin before and after detector switches were omitted
5. data with sudden SUD changes larger than 3σ (about 250 counts/128 s) were rejected
6. data from orbits passing through the South Atlantic Anomaly were rejected

2.2. Light curve

We have fitted linear relations $C = a + bt$ to the data of each day, where C is the observed count rate, t is time (s) and a and b are constants to be determined (Table 1). There was no need to include quadratic or higher order terms. For each day, we have taken the zero point of the time scale at the centre of the time interval where data were present. In general, the statistical error on a is small compared to the error in b; therefore we list the ratio b/a with its error in Table 1: if the variability in all energy bands was similar, then the energy bands should have the same b/a within the statistical errors. Moreover, if we define the characteristic variability time scale τ by

$$\frac{1}{\tau} \equiv \frac{1}{C}\frac{dC}{dt} \qquad (1)$$

we find that $\tau = 1/(b/a)$ at the centre of the interval ($t=0$).

The light curve of 3C 382 is shown in Fig. 1. We give light curves in 2 energy bands: the low energy band from 1.1 – 2.2 keV, and the high energy band, from 2.2–9.7 keV. From this figure and Table 1, we note the following:

1. Variability is present in our data. The maximum variability range is 40% for the low energy range and 35% for the high energy range. Quoted values correspond to maximum count rate compared to minimum count rate.
2. The typical variability time scale is of the order of a day for both energy ranges. The fastest time scale present in the data is $\tau = 1$ day (rise time, low energy) and $\tau = 2$–3 days (decay time, high energy).
3. There is no evidence for a correlation of the variability in both energy bands, although time scales and amplitudes are similar. In particular, the count rate in the high energy band decreases significantly during 21 July, while the low energy band count rate remains constant or even increases; similarly, at 22 July the low energy band count rate increases while the high energy flux remains constant.

Table 1. Linear fits to the light curve

Day of July	a c/s	b/a 10^{-6} s	τ 1000 (s)
	1.1 – 2.2 keV:		
20	0.56 ± 0.02	-2.4 ± 3.5	
21	0.58 ± 0.02	3.0 ± 3.5	
22	0.59 ± 0.02	11.7 ± 3.5	85 ± 25
23	0.56 ± 0.03	-3.7 ± 18.1	
	2.2 – 9.7 keV:		
20	4.69 ± 0.05	-3.8 ± 1.1	-263 ± 79
21	4.10 ± 0.06	-6.2 ± 1.4	-161 ± 35
22	4.35 ± 0.05	-0.7 ± 1.3	
23	4.33 ± 0.09	-4.0 ± 6.4	

4. An inspection of Fig. 1 shows that if any correlation between the count rates in both bands should exist, the count rates in one energy band should be delayed with respect to the other by at least half a day. We stress however, that this is only a lower limit; due to gaps in the present data set we have insufficient evidence to prove or disprove correlations on such time scales.

5. Rebinning the data into other energy bands shows that 2 keV is indeed the boundary between the different time behaviour at low and high energies.

2.3. *Spectrum*

We fitted the present data with different spectral models. Components used are ($F(E)$ denotes the spectrum in photons $m^{-2}s^{-1}keV^{-1}$, where E is the photon energy in keV):

power law $F(E)=CE^{-\Gamma}$

delta line $F(E)=C\delta(E-E_0)$

blackbody $F(E)=CE^2/(e^{E/T}-1)$

thermal bremsstrahlung $F(E)=Ce^{-E/T}G(E,T)/E$

where E_0 and T are all in keV, and $G(E,T)$ is the Gaunt factor taken from Matteson (1971).

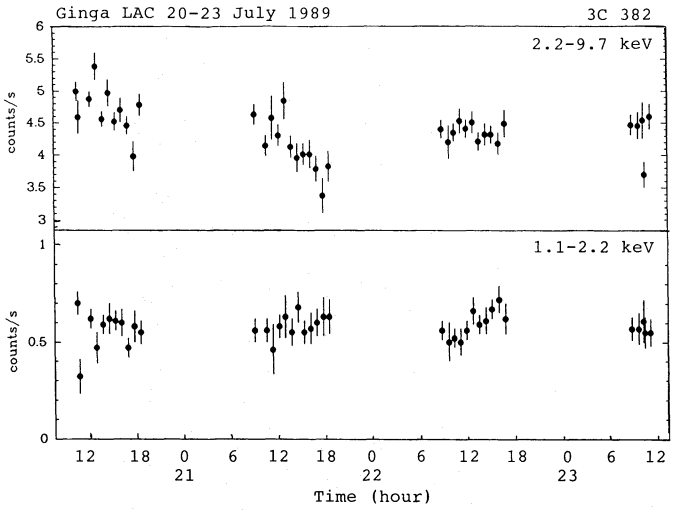

Fig. 1. Light curve of 3C 382. Lower panel: 1.1–2.2 keV. Upper panel: 2.2–9.7 keV

The results of our spectral fits are given in Table 2. Parameters enclosed in brackets ( ) were held constant during the fitting procedure. Errors denote 90% errors for one interesting parameter (cf. Lampton et al. 1976). For the interstellar absorption cross sections we used the data of Morrison & McCammon (1983).

Model 1 is a simple power law with the absorbing column density left free. In model 2 we fix the column density to the value for our own galaxy (Heiles 1975). Since model 1 yields a very low column density, but is consistent with model 2 (the fits have nearly the same χ^2), we will adopt the galactic value of $8\ 10^{24}\ m^{-2}$. This value is also consistent with the well known fact that high luminosity AGN like 3C 382 suffer little from internal absorption (e.g. Mushotzky 1984). Moreover, runs made with partial covering models did not result in a better fit.

Inclusion of an Fe-line improves the goodness-of-fit considerably, as a comparison of model 3 with model 2 shows. The improvement is significant at the 1.2% significance level.

A further significant reduction of χ^2 (at the 0.17–2.4% significance level, depending upon the model) is reached if a soft excess is introduced. This is shown in models 4–6 (Figs. 2–4), where apart from the main power law and the Fe-line either blackbody radiation, thermal bremsstrahlung or a soft power law are introduced respectively. Although there are small differences in the goodness-of-fit between these models for the soft excess, it is not well possible to discriminate between these models based upon the present spectral fits.

It is evident from Table 2 that the luminosity and power law index of the main power law component depend rather heavily upon the adopted shape of the soft excess. Moreover, even given a particular model for the soft excess, there exist strong correlations between the parameters. For example, if we adopt model 4 (blackbody), then for the lowest acceptable (90% confidence level, taking 5 interesting parameters) blackbody temperature of 0.10 keV the power law index is 1.49, while for the highest value of 0.67 keV the power law index is 1.25; similarly, the 2–10 keV luminosity of the power law changes from $1.9\ 10^{37}$ W to $1.6\ 10^{37}$ W.

In Table 3 we list the luminosities for the components of the different models, reduced to the rest frame of 3C 382 using its cosmological redshift of 0.0586 (Schmidt 1965). For the power law components, we list the 2–10 keV luminosity, while for the Fe-line and the blackbody or thermal bremsstrahlung component we list the bolometric luminosity.

Finally, we investigated the four spectra of the separate days in order to look for spectral variability. We discuss here model 4

Table 2. Spectral fits

Mod. nr.	χ^2	d.o.f.	N_H (10^{24} m^{-2})	PL Γ	C (photons $m^{-2}s^{-1}keV^{-1}$)	Line E_0 (keV)	C (photons $m^{-2}s^{-1}$)	Soft comp. Γ or T(keV)	C (photons ($m^{-2}s^{-1}keV^{-1}$)
1	33.04	18	0	1.47 ± 0.01	21.8 ± 0.3				
2	34.89	19	(8)	1.49 ± 0.05	22.6 ± 1.7				
3	25.96	17	(8)	1.51 ± 0.05	22.3 ± 1.6	6.24 ± 0.30	0.36 ± 0.17		
4	15.09	15	(8)	1.34 ± 0.12	15.9 ± 3.9	6.16 ± 0.25	0.40 ± 0.18	0.44 ± 0.14 (BB)	49 ± 60
5	18.52	15	(8)	1.46 ± 0.03	20.3 ± 0.9	6.22 ± 0.27	0.35 ± 0.15	0.34 ± 0.06 (TB)	5100 ± 6100
6	13.14	15	(8)	1.03 ± 0.04	6.6 ± 0.6	6.18 ± 0.21	0.42 ± 0.15	2.33 ± 0.11 (PL)	26.6 ± 2.6

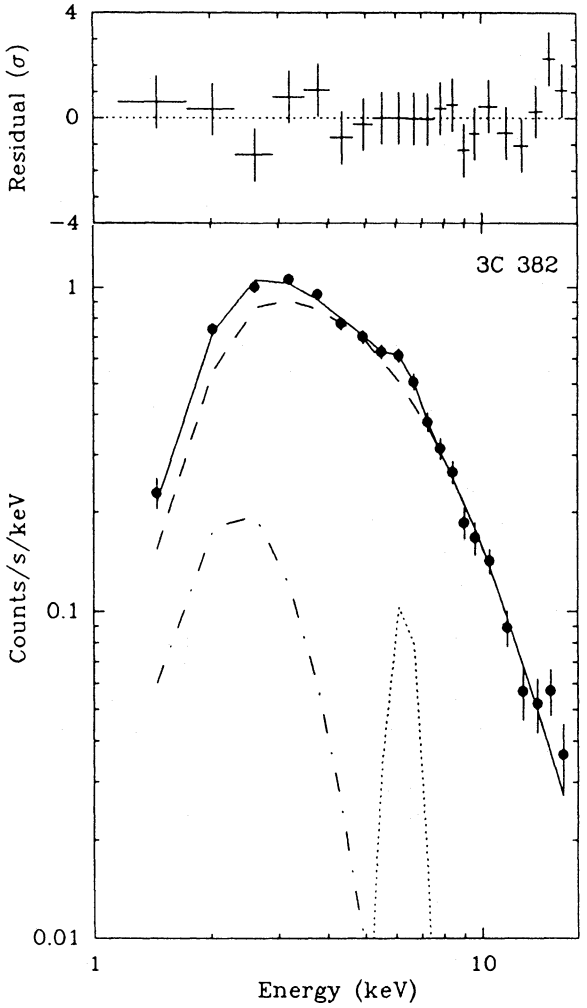

Fig. 2. Ginga LAC spectrum of 3C 382. Lower panel: observed count rate spectrum of 3C 382. Dashed line: power law component; dotted line: Fe-line; dash-dotted line: soft excess, fitted by a blackbody model; continuous line: total model spectrum. Upper panel: fit residuals, expressed in units of the observed standard deviation; the error bars are all 1σ

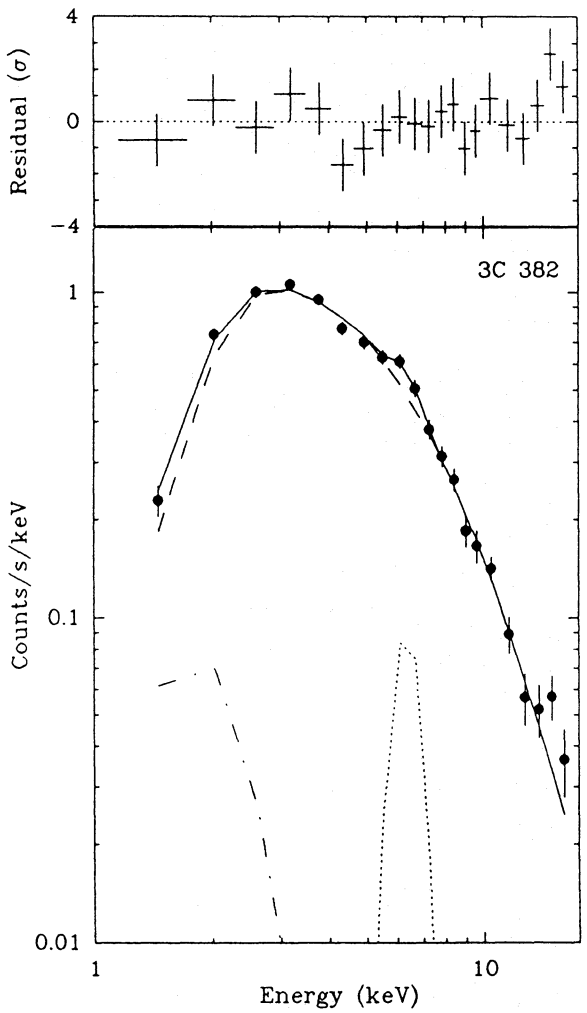

Fig. 3. Ginga LAC spectrum of 3C 382. As Fig. 2, but here with thermal bremsstrahlung as the model for the soft excess

(power law, line and blackbody) but the results with model 5 and 6 are similar. We found no significant changes of the spectral shape parameters for the components, i.e. Γ is constant within a factor of 0.14 (all values quoted here are 1σ), E_0 within 0.2 keV and T is constant within 0.15 keV. These limits are relatively large due to the strong intercorrelation of some parameters (in particular Γ and T).

By fixing the 3 spectral shape parameters at the average value for the 4 days (Table 3), allowing only for variations in the normalisations, we find evidence for variability of the power law flux consistent with the light curve (Fig. 1). The statistics of the Fe-line however are to poor to discriminate between constancy of the line and variations proportional to the continuum flux. From day to day, the variations in the average blackbody flux are very small; note however that the light curve shows evidence for significant changes during some days.

3. Discussion

3.1. Power law component

The best fitting spectra obtained by the LAC indicate the presence of 3 spectral components: a power law, an Fe-line and a soft excess.

The hard X-ray luminosity of 3C 382 was very low during the present observation (see Fig. 5). It was 50% lower than the minimum of all previous reported luminosities. Only the Ariel V measurement in 1975 had a comparable luminosity, although this measurement was only a $3\text{–}5\sigma$ detection.

The fastest observed decay time of the hard X-ray flux was 2 days (Table 1). This is 2.3 ± 0.4 times faster than the variability time reported by Barr & Mushotzky (1986) using EXOSAT data. However, the luminosity during that EXOSAT observation was 3.1 times larger than during the present Ginga observations, so the data are consistent with a linear relation between variability time scale and 2–10 keV luminosity for 3C 382, similar to the correlation found by Barr & Mushotzky among a sample of many AGN.

Subtracting the linear trends corresponding to the 2 days variability from the data and considering the residuals imposes an

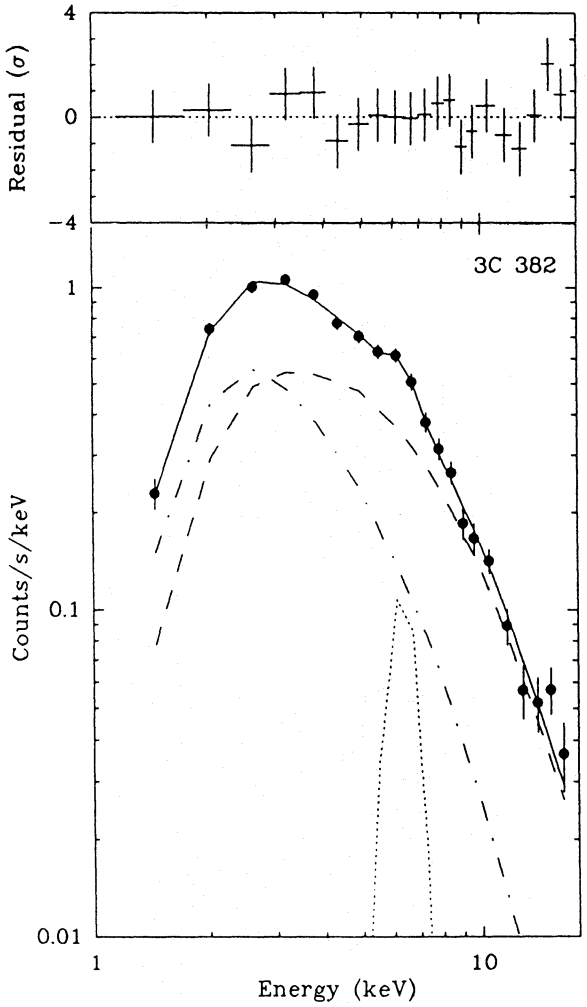

Fig. 4. Ginga LAC spectrum of 3C 382. As Fig. 2, but here with a second power law as the model for the soft excess

Table 3. Rest-frame luminosities of the spectral components (units: 10^{35} W)

Model	Power-law	Fe line	Soft comp.
1	199	—	—
2	201	—	—
3	192	5.7	—
4	180	6.3	32 (BB)
5	190	5.5	10 (TB)
6	121	6.7	69 (PL)

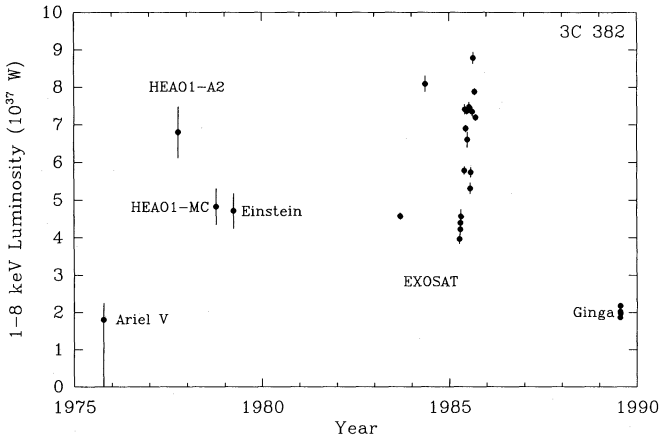

Fig. 5. Long time scale X-ray light curve of 3C 382. Data from Ariel V (Elvis et al. 1978), HEAO-1 A-2 (Marshall et al. 1979), HEAO-1 MC (Dower et al. 1980), Einstein (SSS and MPC data averaged) (Petre et al. 1984), EXOSAT ME (from EXOSAT database, see also Barr 1990), and Ginga (present work). All data are reduced to the 1–8 keV band

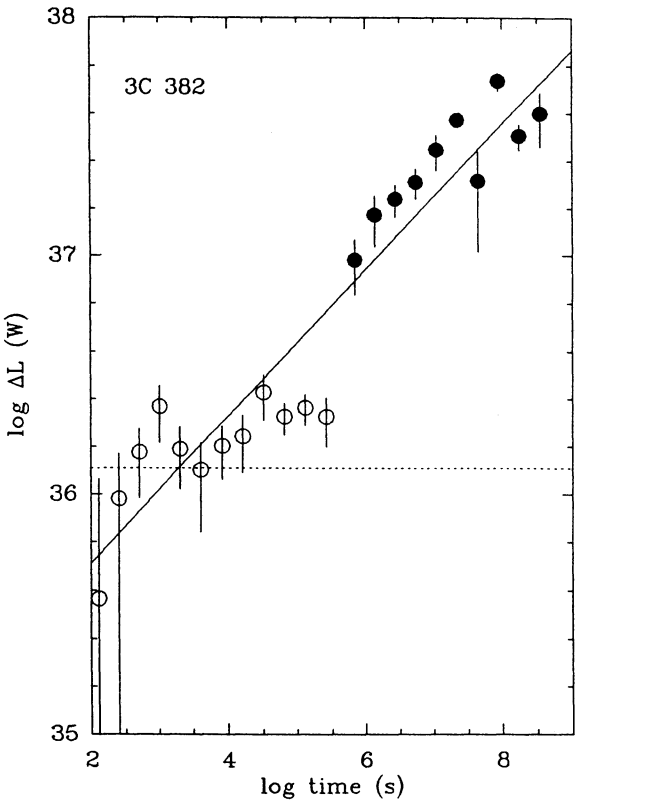

Fig. 6. Root-mean-squared luminosity changes in the 1–8 keV band as a function of time difference in 3C 382. Open symbols: using present Ginga data; solid symbols: from Fig. 5. The dotted line indicates the confusion limit of the LAC; the solid line represents the best fit power law to the data

upper limit 4% to any rms variability on time scales of 128 s to 2 days. This shows that the 2 days time scale is probably indeed the fastest time scale present in 3C 382.

Figure 6 shows the root-mean-squared luminosity changes as a function of time delay, using a method similar to the cross-correlation method of Edelson & Krolik (1988): by combining all possible pairs of data (L_i, L_j), sorting them with respect to increasing time difference $|t_i - t_j|$ and calculating the RMS of the luminosity difference $|L_i - L_j|$, for all data within a certain time difference range. We applied the method to 2 data sets: the long time scale light curve of Fig. 5 and the present Ginga data, binned into 128 s bins. Note that the method is sensitive to systematic

errors due to undersampling of the light curve: e.g., it is clear from Fig. 1 that the minima and maxima in the Ginga light curve occurred during times when no measurements were done; therefore the real RMS changes on a time scale of 1 day could be a factor of ~ 2 larger. Nevertheless it is clear from Fig. 6 that there is increasing variability for increasing time scales, from at least 10 000 s (below that time scale the confusion limit of Ginga is reached) up to at least one year or maybe even up to 10 yr. Note that the luminosity differences on a time scale of 10 000 s are probably due to the gradual 2 day variations.

The maximum radius of the hard X-ray source using the light travel time and the observed decay time of 2 days is $4.8\ 10^{13}$ m. If we assume that the hard X-ray source is located at 5 Schwarzschild radii, then the central mass is $\lesssim 3.3\ 10^9\ M_\odot$. The total detected radio, IR–UV and X-ray luminosity is at least $1.5\ 10^{38}$ W (see Fig. 7). If that luminosity is smaller than the Eddington luminosity, the central mass of 3C 382 is $\gtrsim 1.2\ 10^7\ M_\odot$.

A probably more realistic mass estimate is obtained if we identify the fastest observed variability time scale of 2 days with the thermal instability time scale at 5 Schwarzschild radii in a thin accretion disk surrounding the central black hole. This has been proposed for e.g. NGC 5548 by Kaastra & Barr (1989). Assuming a value for the disk parameter $\alpha = 0.1$ the observed time scale implies a central mass of $1.0\ 10^8\ M_\odot$, well within the limits discussed before. The observed luminosity of 3C 382 in the IR–UV and X-ray region is then some 10–20% of the Eddington luminosity. This number may be even higher if a considerable energy output exists in the far EUV/soft X-ray or the γ-ray region of the spectrum.

If the power spectrum of the variations is limited by the thermal and the viscosity time scale in the disk, then the increasing variability up to at least a time scale of a year would imply an accretion rate of at most $0.1\ M_\odot\ \mathrm{yr}^{-2}$. In that case the disk would be thin. Since the basic mechanisms behind the variability are yet largely unknown, these estimates must be considered tentatively. However comparing the UV bump spectrum of 3C 382 (Fig. 7) with the accretion disk models of Czerny & Elvis (1987), we also obtain a typical mass of $10^8\ M_\odot$ and an accretion rate of $0.1\ M_\odot\ \mathrm{yr}^{-1}$, both within a factor of ~ 3.

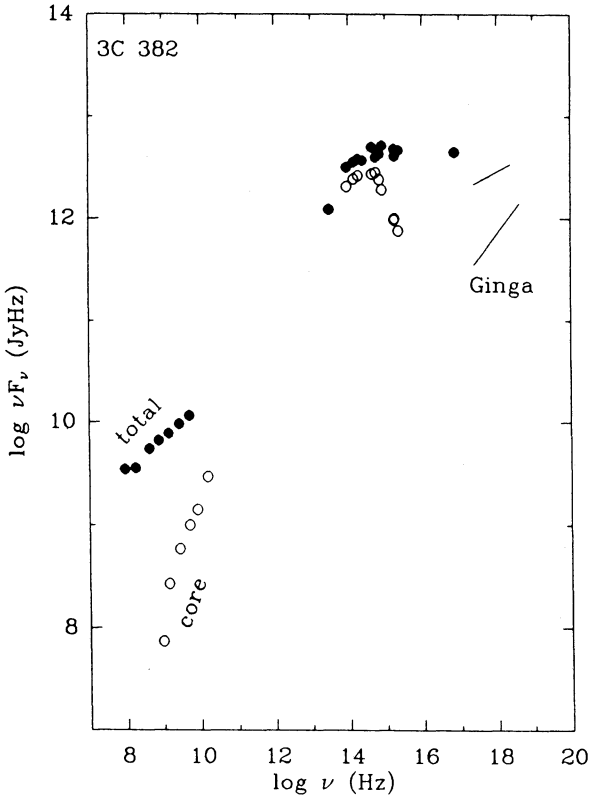

Fig. 7. Continuum flux distribution in 3C 382. Radio frequencies, open symbols: core flux; solid symbols: core + lobes. IR–UV, open symbols: minimum flux observed; solid symbols: maximum flux. X-rays, upper line: maximum X-ray spectrum observed by the EXOSAT ME detector; lower line: Ginga LAC spectrum. Solid dot at soft X-rays: EXOSAT LE flux (same epoch as the plotted ME flux), assuming blackbody radiation of 0.05 keV at the effective detector energy of 0.3 keV, plus the power law component. Radio data from MacDonald et al. (1968), Kellerman et al. (1969), Conway et al. (1972), Riley & Branson (1973), Bridle & Fomalont (1978), Strom et al. (1978), Burch (1979a), Kerr et al. (1981), Parma et al. (1986), Rudnick et al. (1986). IR-optical data from Puschell (1981), UV from Tadhunter et al. (1986), X-rays from the EXOSAT database (see also Barr 1990) and from the present work

3.2. Fe-line

The observed energy of the Fe-line reduced to the rest frame of 3C 382 is 6.52 ± 0.26 keV. We interpret this line as due to fluorescence in dense material in the neighbourhood of the central X-ray source. The observed line energy is consistent with both cool and hotter material (6.4–6.7 keV). The equivalent width of 280 eV (derived from Table 2) is rather large: it was smaller for a sample of 12 Seyferts observed by Ginga (Pounds 1989).

The equivalent width of the fluorescent Kα line for a power law continuum in a photo-ionised, optically thin (with respect to electron scattering) medium is given by formula (3) of Krolik & Kallman (1987):

$$EW = \varepsilon_\alpha Y [0.67 f(\Xi) \tau_{es}] f_{coc}/(2+\Gamma) \qquad (2)$$

where ε_α is the energy of the Kα line, Y is the fluorescence yield, $f(\Xi)$ is a function of Ξ, the ionisation parameter, τ_{es} is the electron scattering depth, Γ the photon index of the power law spectrum and f_{cov} is the covering factor of the fluorescent material. For cool unphotoionised material ($\Xi = 0$) it follows from the equivalent width of 280 eV and the maximum value of $\tau_{es} = 1$ that the covering factor is 0.38; the result is rather insensitive to the value of Ξ, but for lower values of τ_{es} the covering factor would be even higher.

The high covering factor could be due to the presence of an accretion disk. But why is the equivalent width in 3C 382 so large compared to other active nuclei? First we note that the jets of 3C 382 probably have a large inclination angle i: both from the observed length and intensity ratio of the NE and SW radio lobes, a value of $\beta \cos i = 0.10 \pm 0.02$ is deduced; for β not too small, large inclination angles are therefore required. Thus we might see the accretion disk roughly edge-on. Such a large inclination could also explain the very broad Balmer and UV lines in 3C 382 if the broad line clouds have a considerable rotational component. Secondly, for a sample of 9 superluminal quasars, where we probably look at a face-on disk, no Fe-line was observed (Ohashi 1989). So there could be a correlation between equivalent width of the Fe-line and inclination angle. The possible origin for such a correlation and more observational evidence for its presence is beyond the scope of this paper.

The apparently large equivalent width may also be due to missing continuum flux. This is probably the case for the Fe-line in the Seyfert 2 NGC 1068 (Koyama et al. 1989), where only reflected continuum X-rays are observed. For 3C 382 this seems unlikely, since 3C 382 has extremely wide, unabsorbed broad optical lines and the broad line region is larger than the X-ray emitting region. However 3C 382 had a very low X-ray flux during our observation. If the X-ray flux close before the observation was much higher, then time delay effects cause a large equivalent width for any fluorescent material which is at least a few light days from the central source.

3.3. *Soft component*

The spectral shape of the soft component is not well determined due to a limited efficiency and spectral resolution of Ginga below 2 keV. However, since the light curve below and above 2 keV is different, a very soft spectrum of the soft component is more likely. We tested this hypothesis as follows.

For each of the first 3 days of observation (where a long data train exists) we fitted the 1–10 keV data binned into 6 energy bins to a linear function of time (as in Sect. 2). From these fits, the count rate difference of start and end of each observation was determined. The difference spectra for the 3 days generated this way were fitted with the spectra of models 4–6 with the spectral shape parameters fixed to the values obtained from the whole observation, and only the normalisation of the power law and soft component left free. The sum of the χ^2 goodness-of-fit values of the three days is 20.7, 13.5 and 24.9 for the blackbody, bremsstrahlung and soft power law model, respectively; χ^2 has 12 degrees of freedom. The bremsstrahlung spectrum fits best, but the blackbody spectrum cannot be rejected at the 6% level. The soft power law hypothesis is rejected at the 2% significance level. The soft power law model is only acceptable if its slope also varies. This is unlikely given the observed hardness constancy in the 2–10 keV band where the soft power law component contributes significantly and the limited variability amplitude in the 1–2 keV band.

We conclude that the soft component shows a sharp spectral cut-off above 2 keV; its shape is badly determined but it could resemble a blackbody or bremsstrahlung spectrum. Its temperature is in the range of 0.3–0.5 keV. The variability amplitude of the soft excess may be rather large, as the analysis of the previous paragraph shows (Table 4). The corresponding exponential rise times are of the order of 10 000–20 000 s for the bremsstrahlung model and 30 000–50 000 s for the blackbody model, faster than the main power law variations. However in the 1–2 keV band we observe only the (exponential) tail of the soft component. A change of only 20% in temperature results in a flux change of a factor of 2 in this band. So the apparent fast variability of the soft component is illusionary. And indeed we do not observe rapidly succeeding maxima.

Table 4. Variability (%) of the power law and soft component with respect to average flux of each day

Day (1989)	Powerlaw	Soft component	
		Blackbody	Thermal bremsstrahlung
20 July	6 ± 1	0 ± 10	11 ± 22
21 July	9 ± 2	32 ± 11	89 ± 24
22 July	3 ± 1	51 ± 10	121 ± 22

Evidence for a soft excess in 3C 382 is also reported from EXOSAT data (Barr 1990) and Einstein IPC data (Urry 1989). The count rate in EXOSATs LE telescopes of the soft excess and the main power law are comparable. The soft excess has a typical temperature $\lesssim 0.05$ keV and the count rate in the thin lexan filter is 25–70 times larger then the count rate predicted from the present Ginga soft component. The IPC data show a component with a typical temperature of 0.24 keV, which is consistent with the present Ginga observations.

Clearly, the soft excess in 3C 382 in the energy range of 0.05–2 keV as observed by Ginga and EXOSAT is different. Fitting both by a simple one component power law or blackbody is insufficient. Alternatively, with Ginga we could observe the same physical component as EXOSAT observed, if this component is highly variable. We note that both the hard X-ray flux and the soft excess flux were much lower during the present observation than during all EXOSAT observations, but the temperature of the soft excess was higher, and probably also the coronal temperature since our power law spectrum was harder than the average EXOSAT spectrum. In that case a clear anticorrelation between soft X-ray flux and temperature must be present.

An interesting possibility for the nature of the soft component is inverse Compton scattering in an optically thin (with respect to electron scattering) part of an accretion disk corona (e.g. Czerny & Elvis 1987). The main power law component could originate in an optically thick part of the corona. In both cases, thermal radiation from the disk constitutes the input of soft photons. In the thick part of the corona, these soft photons scatter repeatedly thus giving rise to the power law with a cut-off in the spectrum near the coronal temperature. In the optically thin part of the corona, photons scatter only once, thus leading to a much softer component. The very soft X-ray component observed by EXOSAT could be the source of soft photons fuelling the corona.

4. Conclusions

Ginga observations of the X-ray spectrum of 3C 382 reveal the following new results.

The continuum X-ray flux during the present observation was 2 times lower than all previous measurements (except perhaps the marginal Ariel V detection in 1975). Hard X-rays (2–10 keV) constituted probably less than 10% of the bolometric luminosity of 3C 382. Variability with exponential rise/decay times of 2 days is present. This time scale is consistent with earlier EXOSAT measurements accounting for the difference in luminosity. The amplitude of the variations is rather low: at most 35% (maximum/minimum). The upper limit to the variability at smaller time scales from 128 s to 2 days is 4%. The variability amplitude increases with increasing time scale up to at least 1 yr. At longer time scales variability may possibly have constant amplitude.

If the minimum time scale is identified with the thermal time scale in an accretion disk at 5 Schwarzschild radii, and the maximum time scale of at least a year with the viscosity time scale, a typical black hole mass of $10^8\ M_\odot$ and an accretion rate of $0.1\ M_\odot\ \mathrm{yr}^{-1}$ is deduced. These values are consistent with the UV

spectrum of 3C 382 if compared with the accretion disk models of Czerny & Elvis (1987).

The X-ray spectrum of 3C 382 consists of 3 components: a power law, an Fe-line and a soft excess. The spectral shape of these 3 components does not vary significantly during 4 days of observation.

The energy of the Fe-line (6.5 ± 0.3 keV) is consistent both with cool and hotter fluorescent material. The large equivalent width of the line may be due to reprocessing in a nearly edge-on accretion disk. Another explanation would be delay effects in a region more than 1 light week from the central source, which in that case should exhibit a gradual factor of 2 decrease in at least a week.

The spectral shape of the soft component is poorly determined; from its variability properties we deduce that it has a strong cut-off near 2 keV. It has a much lower flux but a much higher temperature than the soft excess detected by EXOSAT. Considering also the very low overall flux during the present observation, an anticorrelation between flux and (disk) temperature is probably present in 3C 382. We suggest the possibility that the presently observed soft excess is due to inverse Compton scattering in an optically thin part of the accretion disk corona, while the hard X-ray power law component is produced in an optically thick part of the corona. The very soft excess as observed by e.g. EXOSATs LE detector could be the source of scattering photons. The variability time scale of the soft excess is similar to the time scale of the main power law component. Delays of at least half a day of one component with respect to the other can be present in the data but cannot be proved.

Acknowledgements. J.S. Kaastra thanks staff and students of the Astrophysics Department of Nagoya University for their hospitality during his stay at Nagoya. The Laboratory for Space Research Leiden is supported financially by NWO, the Netherlands Organization for Scientific Research.

References

Barr P., 1990 (in preparation)
Barr P., Mushotzky R.F., 1986, Nat 320, 421
Bridle A.H., Fomalont E.B., 1978, AJ 83, 704
Burch S.F., 1979a, MNRAS 186, 293
Burch S.F., 1979b, MNRAS 186, 519
Conway R.G., Gilbert J.A., Kronberg P.P., Strom R.G., 1972, MNRAS 157, 443
Czerny B., Elvis M., 1987, ApJ 321, 305
Dower R.G., Griffiths R.E., Bradt H.V., Doxsey R.E., Johnston M.D., 1980, ApJ 235, 355
Edelson R.A., Krolik J.H., 1988, ApJ 333, 646
Elvis M., Maccacaro T., Wilson A.S., Ward M.J., Penston M.V., Fosbury R.A.E., Perola G.C., 1978, MNRAS 183, 129
Hayashida K., Inoue H., Koyama K., Awaki H., Takano S., Tawara Y., Williams O.R., Denby M., Stewart G.C., Turner M.J.L., Makishima K., Ohashi T., 1989, PASJ 41, 373
Heiles C., 1975, A&AS 20, 37
Kaastra J.S., Barr P., 1989, A&A 226, 59
Kellerman K.I., Pauliny-Toth I.I.K., Williams P.J.S., 1969, ApJ 157, 1
Kerr A.J., Birch P., Conway R.G., Davis R.J., Stannard D.S., 1981, MNRAS 197, 921
Koyama K., Inoue H., Tanaka Y., Awaki H., Takano S., Ohashi T., Matsuoka M., 1989, PASJ 41, 731
Krolik J.H., Kallman T.R., 1987, ApJ 320, L5
Lampton M., Margon B., Bowyer S., 1976, ApJ 208, 177
MacDonald G.H., Kenderdine S., Neville A.C., 1968, MNRAS 138, 259
Marshall F.E., Mushotzky R.F., Boldt E.A., Holt S.S., Rothschild R.E., Serlemitsos P.J., 1978, Nat 275, 624
Marshall F.E., Boldt E.A., Holt S.S., Mushotzky R.F., Pravdo S.H., Rothschild R.E., Serlemitsos P.J., 1979, ApJS 40, 657
Matteson J. L., 1971, An X-ray survey of the Cygnus region in the 20 to 300 keV range, Thesis, University of California, San Diego
Morganti R., Fanti R., Gioia I.M., Harris D.E., Parma P., de Ruiter H., 1988, A&A 189, 11
Morrison R., McCammon D., 1983, ApJ 270, 119
Mushotzky R.F., 1984, in: X-ray and UV emission from Active Galactic Nuclei, eds. W. Brinkmann, J. Trümper, MPE report 184, Garching FRG, p.73
O'Dell S.L., Puschell J.J., Stein W.A., Warner J.W., Ulrich M.-H., 1978, ApJ 219, 818
Ohashi T., 1989, in: Proceedings of the 23rd ESLAB symposium, ed. ESA, ESA SP-296, p. 837
Osterbrock D.E., Koski A.T., Phillips M.M., 1976, ApJ 206, 898
Osterbrock D.E., Koski A.T., Phillips M.M., 1975, ApJ 197, L41
Parma P., de Ruiter H.R., Fanti C., Fanti R., 1986, A&AS 64, 135
Petre R., Mushotzky R.F., Krolik J.H., Holt S.S., 1984, ApJ 280, 499
Pounds K., 1989, in: Proceedings of the 23rd ESLAB symposium, ed. ESA, ESA SP-296, p. 753
Preuss E., Fosbury R.A.E., 1983, MNRAS 204, 783
Puschell J.J., 1981, AJ 86, 16
Reichert G.A., Wu C.-C., Bogess A., Oke J.B., 1985, BAAS 17, 578
Riley J.M., Branson N.J.B.A., 1973, MNRAS 164, 271
Rudnick L., Jones T.W., Fiedler R., 1986, AJ 91, 1011
Schmidt M., 1965, ApJ 141, 1
Strom R.G., Willis A.G., Wilson A.S., 1978, A&A 68, 367
Tadhunter C.N., Pérez E., Fosbury R.A.E., 1986, MNRAS 219, 555
Turner M.J.L., Thomas H.D., Patchett B.E., Reading D.H., Makishima K., Ohashi T., Dotani T., Hayashida K., Inoue H., Kondo H., Koyama K., Mitsuda K., Ogawara Y., Takano S., Awaki H., Tawara Y., Nakamura N., 1989, PASJ 41, 345
Urry C.M., 1989, in: Proceedings of the 23rd ESLAB symposium, ed. ESA, ESA SP-296, p. 789
Yee H.K.C., Oke J.B., 1978, ApJ 226, 753
Yee H.K.C., Oke J.B., 1981, ApJ 248, 472